An Experimental Study on Flow Characteristics of ERF Between Two Parallel-Plate Electrodes by Using PIV Technique

Tae-Hyun Chang*

Division of Mechanical and Automation Engineering, Kyungnam University,
449 Wolyoung Dong, Masan, Kyungnam 631-701, Korea

Sung-Cheol Jang

Department of Mechanical Engineering, Kyungnam University Graduate School,
449 Wolyoung Dong, Masan, Kyungnam 631-701, Korea

An experimental investigation was performed to study the characteristics of ER(Electro-Rheological) fluid flow in a horizontal rectangular tube with or without D. C voltage. To determine some characteristics of the ER flow, 2D PIV(Particle Image Velocimetry) technique was employed for velocity measurements. This research found the mean velocity distributions with 0kV/mm, 1.0kV/mm and 1.5kV/mm for Re=0, 0.62, 1.29 and 2.26. When the strength of the electric field increased, the cluster of ERF was clearly strong along the test tube and the flow rate decreased. The present results will contribute to the economical and compact design of ER fluids system.

Key Words : Electro-Rheological Fluids, Cluster, Particle Image Velocimetry Abstract

Nomenclature

A : Cross-sectional area of the test tube
b : Electrode width
E : Electric field
H : The width of the test tube
L : The length of the test tube
$\dot{m}$: Mass flow late
ΔP : Pressure drop
u : Axial velocity
U_m : Mean axial velocity
τ : Shear stress of ER fluid
μ : Viscosity of ER fluid without electric field
τ_y : Yield shear stress of ER fluid
h : Electrode gap
a, β : Experimental coefficients

* Corresponding Author,
  E-mail : changtae@kyungnam.ca.kr
  TEL : +82-55-249-2613; FAX : +82-55-249-2617
  Division of Mechanical and Automation Engineering,
  Kyungnam University, 449 Wolyoung Dong, Masan,
  Kyungnam 631-701, Korea. (Manuscript **Received**
  March 9, 2004; **Revised** August 4, 2004)

1. Introduction

Recently, many studies have investigated the behavior of ER fluids which depend on rheology that is closely related to the intensity of electric fields. These studies can be applied to robotics area because the response period of ER fluids is within several tenths of msec. Therefore, in addition to the studies by Wang et al. (1989), Simmonds (1991), Brooks (1992), Tsukiji (1996), Yokota et al. (1996) and Youn-Sik Jeon (1998) on the applications of ER fluid to new areas, fundamental studies that confirm the mechanism related to the ER fluid flow characteristics have become important. But only a few studies have investigated ER fluid flow conditions. It is very important to investigate the ER fluid flow conditions to improve the performance of the equipment and systems that use ER fluid.

One study on the flow conditions of ER fluid, Wang et al. (1989) explained the flow characteristics of ER fluid using the numerical analysis method. Tsukiji et al. (1996) calculated using

fundamental equations, which assume that ER fluid behaves like a Bingham fluid. Park Myung Kwan et al. (1999) performed flow visualization experiments for ER fluid in the narrow space between electrodes. Jang et al. (2003), Nakano et al. (1994) and Choi et al. (1994) carried out a fundamental study and visualization experiment of the ER fluid through a dispersion meter, and then a performance test using application apparatus such as ER valves and so on.

As mentioned above, previous studies facussed on flow visualization of the cluster formation of ER fluid between short electrodes (10mm) and narrow clearances (1mm). But, because long electrodes of ER valves and similar equipment produce the ER effect and the ER particle sizes between electrodes are different, experimental investigation on the mechanism of electrical rheology is very important.

In this study, the rheology of ER fluid stagnating or flowing through a dispersion meter will be investigated using the PIV method. And then the ER effect, which appears at the ER valves and their appliance will be observed.

2. Flow Characteristics of ER Fluid

When the inertia force arising from the fluid movement is applied to the ER fluid being charged by an electric field, there is a resistance force acting on the ER fluid. When the coherent force of the ER fluid particles in the electric field is less than the inertia force due to ER fluid movement, the ER fluid, starts to flow, and complicated changes occur near the flow initiation point. These phenomena can not be explained precisely because they generally depend on the size, shape, and temperature of the ER fluid particles, the type of insulation oil, and the intensity of the electric field. The cluster shape depends on the change in flow velocity and the intensity of the electric field so that the shear force may be changed. If the form processes and behaviors of the cluster are investigated and can be evaluated against the flow velocity and electric field intensity changes, the information can be used as the

basic data of ER fluid.

In case there is no electric field the ER fluid acts as Newtonian fluid, but if an electric field is present the ER fluid particles form clusters and take on the characteristics of Bingham fluid, which causes shear stresses to increase. If ER fluid is regarded as Bingham fluid, the relationship between the shear stress and shear velocity ratio of ER fluid can be expressed as follows by Tsukiji et al. (1996).

$$\tau = \tau_y(E) + \mu \frac{du}{dy} = \alpha E^\beta + \mu \frac{du}{dy} \qquad (1)$$

where $\tau_y(E)$ means the yield shear force under an electric field ; μ is the fluid viscosity ; $\frac{du}{dy}$ is the shear velocity ratio ; E is the intensity of the electric field ; α, β are experimental values that depend on the weight fraction ratio, the viscosity of the insulation oil and so on.

Fig. 1 (a) and (b) show the flow characteristics with and without the electric field. With the electric field, the pressure drop is affected by the viscosity of the ER fluid and proportional to the flux between the test tubes. Therefore, the pressure drop can be defined by the as following equation.

$$\Delta P_\mu = \frac{12\mu L Q}{b h^3} \qquad (2)$$

where b is the test tube width, h is the gap between the test tubes, L is the electrode length in the test tube, Q is the flux with no electric field. With no electric field, the ER fluid in the test tube has only viscosity, therefore the flow velocity at the electrodes is zero, and at the other zones a quadratic velocity profile as shown in Fig. 1 (a) is observed. But with an electric field, the pressure drop will be increased by the yield shear stress $\tau_y(E)$ of the ER fluid. Like Fig. 1 (b), it can be regarded as a plug movement of gap h_c between the electrodes, and hence there will be additional pressure drop ΔP_{ER} due to $\tau_y(E)$. This additional pressure drop can be expressed as follows.

$$\Delta P_{ER} = \frac{2L\tau_y(E)}{h} \qquad (3)$$
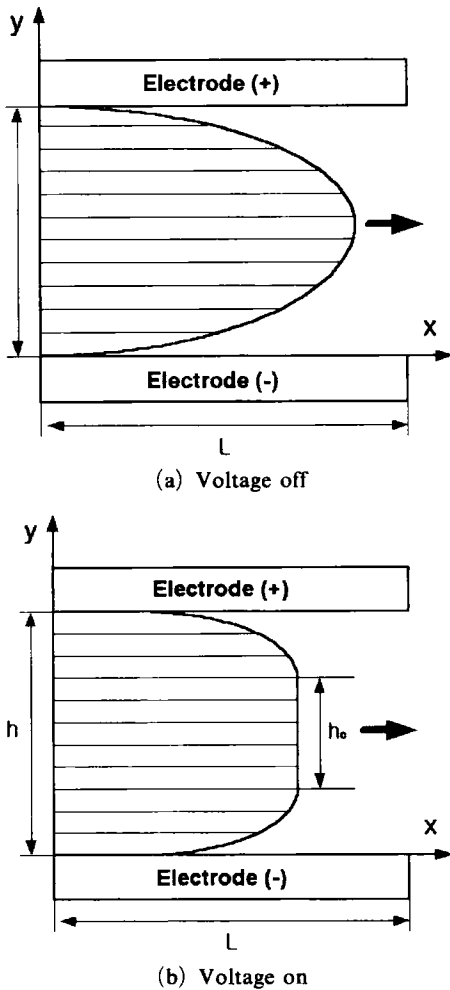
(a) Voltage off

(b) Voltage on

Fig. 1 Flow of ER fluids in the test tube

Here, Q_{ER} represents the flux between the test tube electrodes when the electric field is formed. Although the electric field is formed, if ΔP is less than ΔP_{ER}, there is no flux. But, when the overall pressure drop ΔP is larger than the cluster resistance force, flux exists. Therefore, the overall pressure drop (ΔP) between the test tube electrodes can be defined as the sum of the pressure drop due to the viscosity of the ER fluid and the yield shear stress change according to the electric field.

3. Test Equipment and Method

Fig. 2 shows us a layout of the PIV system and the test equipment, which were used to visualize the flow characteristics of ER fluid mixed with silicone oil and starch particles. They were designed and manufactured to be used for observing the ER fluid in the states of stagnation and flow. ER fluid was stored in a tank, and to prevent it from precipitating and maintain it with uniform composition, the fluid was agitated with an agitator. ER fluid was designed to flow from the tank to the test tube using potential energy. Flux was controlled by valves, which were installed upstream and downstream of the test tube. The ER fluid in test was the ER oil in the dispersion meter, which consisted of silicon oil of S company (ShinEtsu Silicone Korea Co.) and starch particles ($180\mu m$). The test tube was inclined at an angle of 15 degrees to prevent particles from precipitating. In this test, to build up a fully developed flow field in the X-direction, the flow field length was placed as $X/b=60$, and the entrance was designed to minimize an entrance effect. CCD (Charge Couple Device) cameras were installed upstream and at the exit tube. The ER fluid flow could be visualized. The software used in this study was Thinks, which was developed by T Company. The Reynold number was calculated by the average flow speed in the test tube using ER fluid particles speed, the length of the test tube, and the dynamic viscosity of the ER fluid.

Fig. 3 (a) and (b) show the shape of the test tube that was used for visualization of the flow characteristics of the ER fluid. The flow route consisted of a 13mm gap made by 2 electrodes, 240mm in length 25mm in width. To prevent fluid from vaporizing along the route of the test tube, an air vent was installed at the entrance. And the diameter of the entrance and exit was 7mm. The tube was made of transparent acrylic plastic so that the flow inside the tube could be observed using a CCD camera and visual angle. The electrodes were made of copper foil (0.1mm), and installed on the left and right of the tube route. Then, to prevent risk of electric shock from high voltage, the joint area between the test tube base and each components was made of nylon synthetic resin insulator.
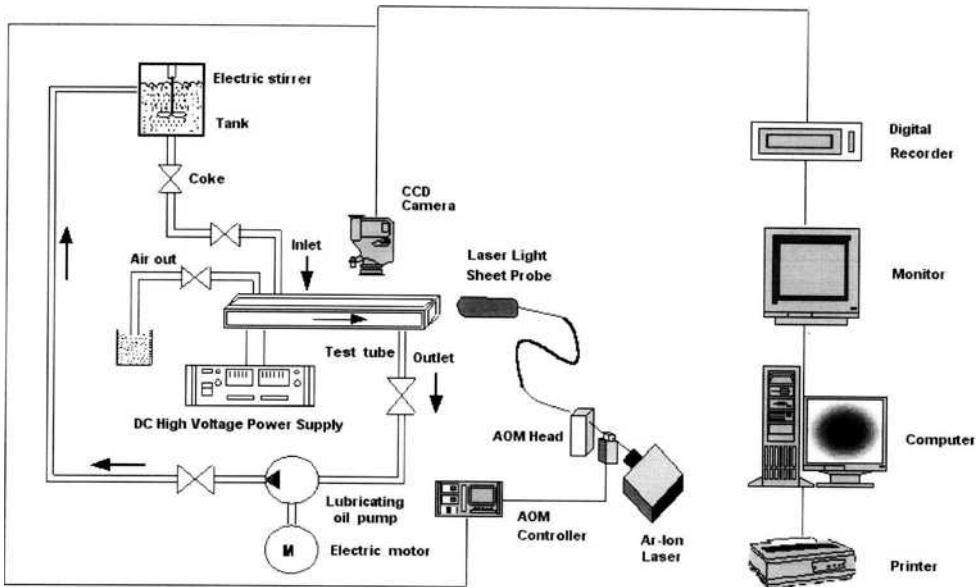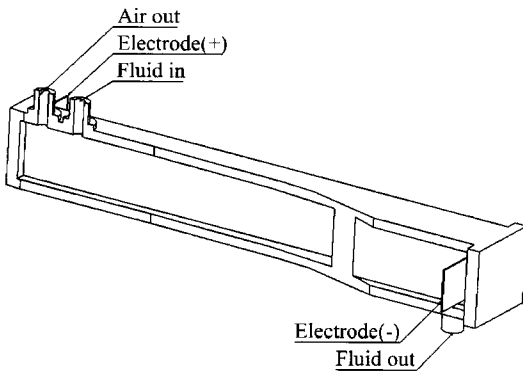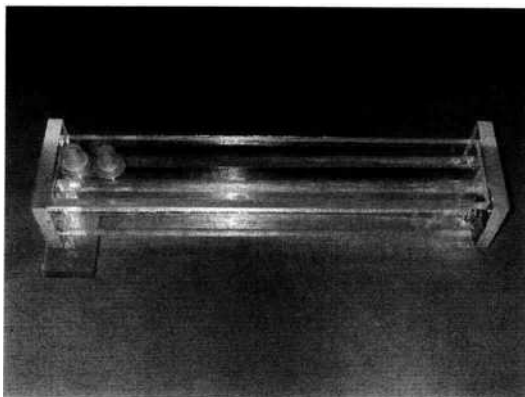
Fig. 2 Experimental apparatus and PIV system

(a) Geometry or the test tube

(b) Photograph of the test tube

Fig. 3 Geometry and photograph of the test tube

4. PIV System

An algorithm in the PTV (Particle Tracking Velocimetry) method saved the particle displacement, using the velocity vector of each particle center and the PIV (Particle Image Velocimetry) method, which uses the relationship of the particle distribution group.
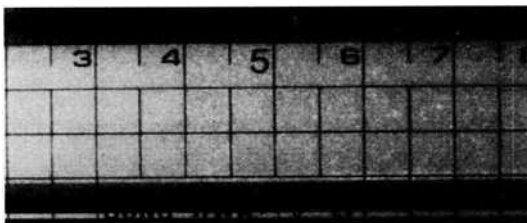
In this study the 2 dimensional PIV method was used. The light source used in the experiment was a 500mW air-cooled Ar-ion laser. To easily shift the light source, LLSP (Laser Light Sheet Probe), which can shift light through an optical cable, was used. Furthermore, this LLSP can control the laser thickness to about 1 mm. The optical cable was about 10 m. To obtain pulsating light source, AOM (Acoustic Optical Modulator) was used. Also, to obtain the flow field image at 30cuts/sec, a CCD camera WV3P310, made by Panasonic Company, was used. Digital recording was used for image recording. And then, to transmit these images to the computer, DT3155 (640×480 pixel) board, at 0 to 225 steps of gray level was used.
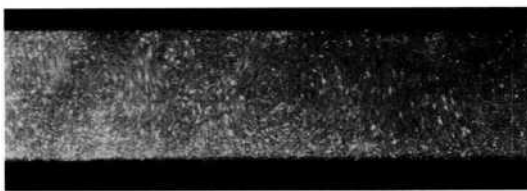
5. Experiment Result and Investigation

5.1 Characteristics of stagnant ER fluid without flow rate

Fig. 4~Fig. 6 are the results of PIV measurement at 1.5kV/mm of electric field, when the exit valve was closed and there was no flow rate (Re=0).
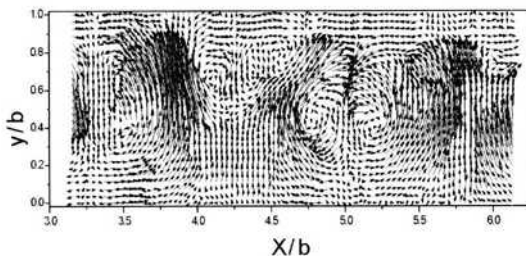
Fig. 4(a) is showing the image before the formation of the electric field. It shows that the ER fluid is uniformly distributed between (+) and (−) electrodes. Fig. 4 (b) shows the same state as Fig. 4(a) but with the formation of the electric field. Both figures show that ER particles shifted to (+) and (−) electrodes and rotated instead of forming a linear cluster. Fig. 4(c) shows the velocity vectors of the ER particle shift. Large shifts occurred at X/b=3.75, 4.2, and X/b=5.7 of the X-direction and y/b=0.4~0.8 of

the Y-direction. This is thought that big ER particles are at X/b=3.75, 4.2, and X/b=5.7 of X-direction and y/b=0.4~0.8 of Y-direction. In this state, with the formation of the electric field, bigger ER particles have bigger ER effects and shift toward (+) and (−) electrodes, and the smaller, stagnated particles may shift minutely because bigger ones push their ways through the smaller ones. After positive and negative charges of ER particles were uniformly distributed and reached equilibrium, and the electric charge formed, the electric charges rotated toward the electrode having the opposite pole, giving the particles momentum and velocity vectors.
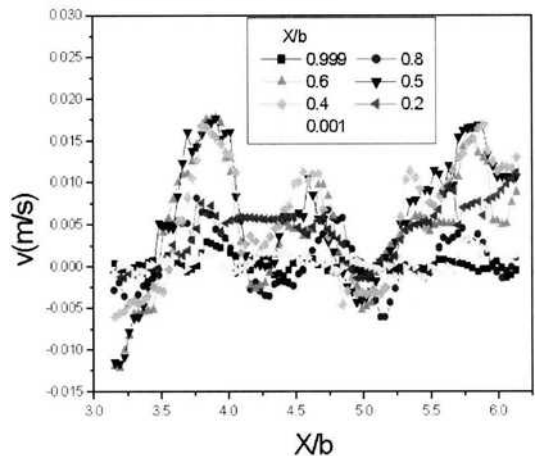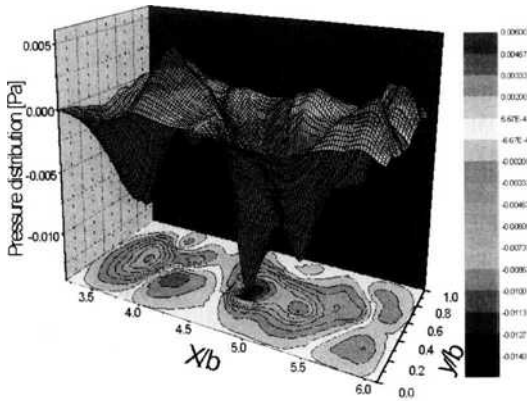

(a) Visualized image (E=0kV/mm)

(b) Visualized image (E=0.8kV/mm)

(c) Mean velocity vectors distributions

Fig. 4 Distributions of ER particles along the test tube for Re=0 with D.C 1.5kV/mm
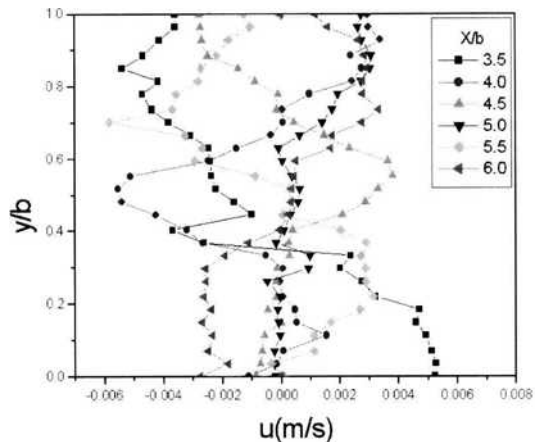
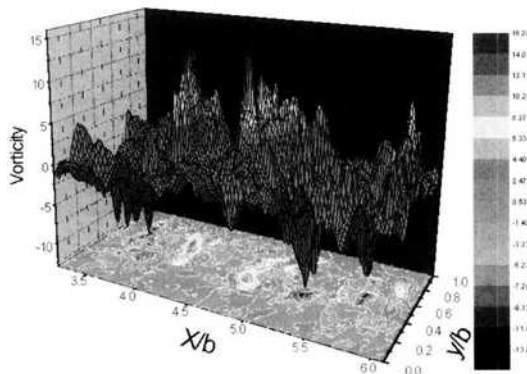

(a) Axial velocity distributions

(b) Radial velocity distributions

Fig. 5 Velocity distributions of ER fluids along the test tube for Re=0 with D.C 1.5kV/mm

(a) Pressure distribution

(b) Vorticity distribution

Fig. 5(a) shows the velocity distribution of ER between X/b=3.5~X/b=6.0 in the X-direction in the state of Fig. 4(c), between y/b=0.0~y/b=1.0 in the Y-direction in the state of Fig. 4(b). ER particles should not have shifted at the electrode length between 0.001 (▶) and 0.999 (■) in the Y-direction, but they shifted. This means that in case of PIV measurement, solid particles adhered to the liquid, and the solid particles were bigger than the liquid particles, therefore solid particles can have an inertia force.

Fig. 6(a) indicates the pressure distribution of ER particles in the state of Fig. 4(c), and Fig. 6 (b) the voltex flow distributions. Fig. 4(c) shows that at 3.75, 4.2, and 5.7 in the X-direction, the speed distribution of the ER particles is high and the pressure is low. The pressure may have decreased in the high-speed zone, and increased at

the low-speed zone.

Fig. 7 shows the flow of ER particles as measured by the PIV method without the formation of the electric field. The velocity vectors obtained by this measurement are shown in Fig. 8. The local velocities calculated from these velocity vectors are shown in Fig. 9. These vectors show a typical laminar flow as in Fig. 1(a). also show the maximum velocity at the center of the tube and the minimum velocity near both walls.

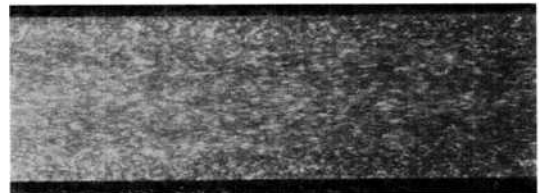## 5.2 Flow characteristics of ER fluid with flow rate

Fig. 7 Distributions of electro-rheogical particles for Re=2.267 along the test tube without D.C voltage
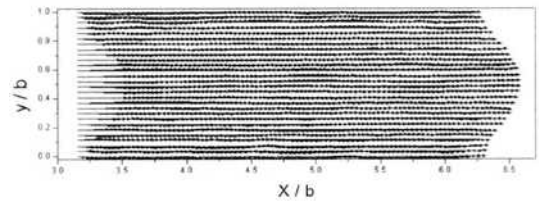

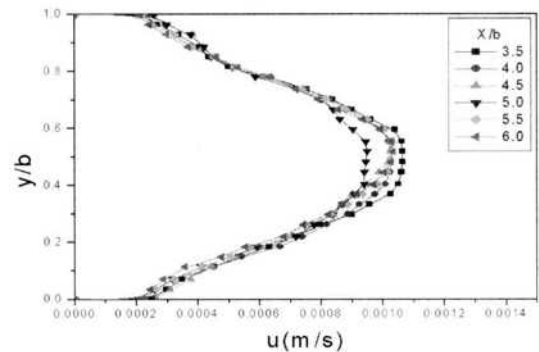**Fig. 8** Mean velocity vector distributions along the test tube for Re=2.267 without D.C voltage

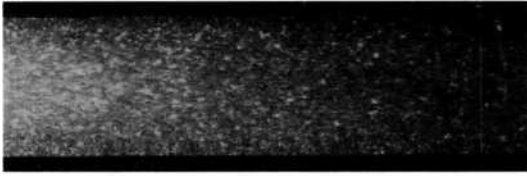**Fig. 9** Velocity distributions along the test tube for Re=2.267 without D.C voltage

Fig. 10 Distributions of electro-rheological particles for Re=2.077 along the test tube with D.C 0.5kV/mm
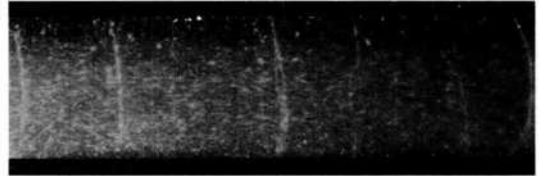

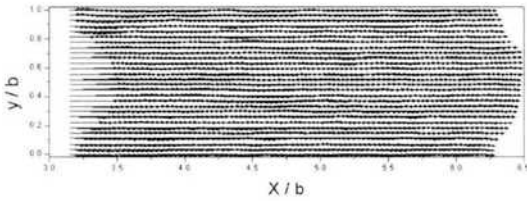**Fig. 11** Mean velocity vectors along the test tube for Re=2.077 with D.C 0.5kV/mm

Fig. 12 Velocity distributions along the test tube for Re=2.077 with D.C 0.5kV/mm

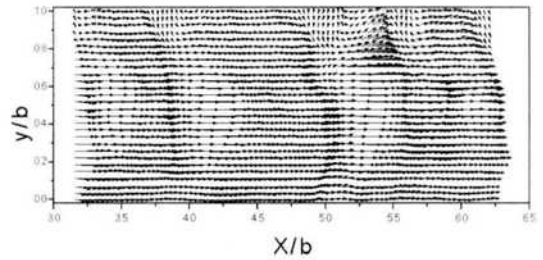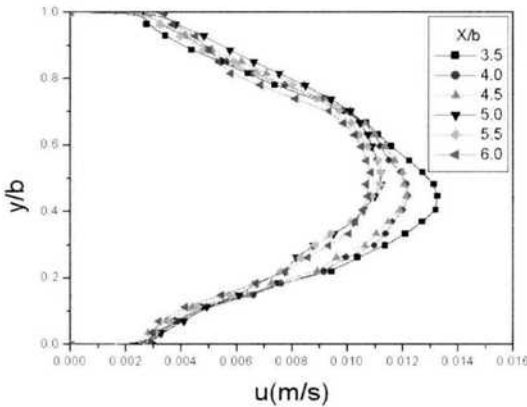**Fig. 13** Distributions of electro-rheological particles

Fig. 14 Mean velocity vector distributions along the test tube for Re=1.29 with D.C 1.0kV/mm
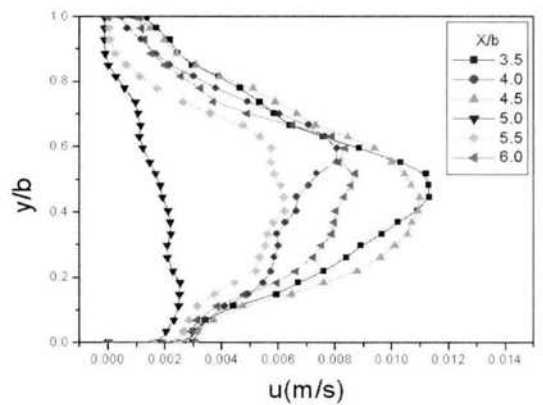

Fig. 15 Velocity distributions along the test tube for Re=1.29 with D.C 1.0kV/mm

mm, is shown in Fig. 10~Fig. 12. Fig. 10 shows no clusters at the forward section of the test tube, but minute clusters at the back section. When the velocity of ER fluid increases, the inertia force becomes greater than the electric force ; Therefore, the clusters are thought to be broken. Fig. 11 and Fig. 12 show that under the same effects, the velocity vectors and local velocity of the ER fluid are not influenced greatly by an electric field. for Re=2.07 along the test tube with D.C 0.5kV/mm.

The ER fluid flow with an electric field 0.5kV/mm, is shown in Fig. 13~Fig. 15. The coherence

of the particles increased, and many clusters, which have a band shape, build up near both electrodes. These clusters change the velocity distribution of the ER fluid, and therefore, the pressure drops at the entrance and exit of the tube. The band type clusters that built up inside the flow route cannot maintain their shapes after the build up but repeat their nullification and creation processes in short cycles. Because of cluster effects due to the electric field, the velocity distribution of the ER fluid increase when ER fluid approaches the lower part.
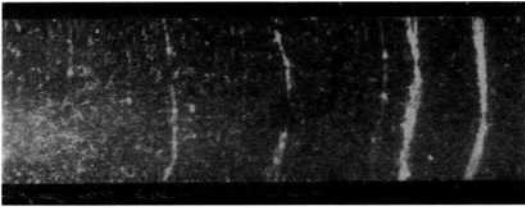
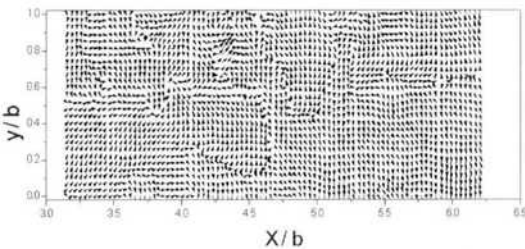Fig. 16   Distributions of electro-rheological particles for Re=0.62 along the test tube with D.C 1.5kV/mm

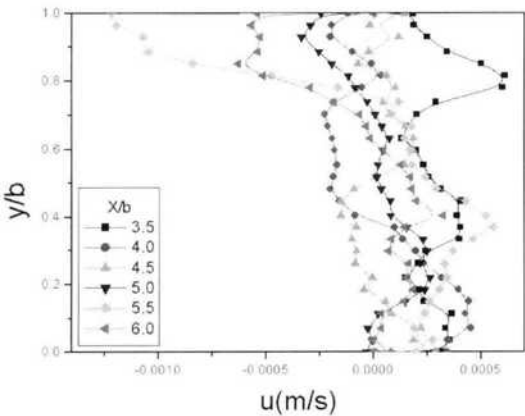Fig. 17   Mean velocity vectors along the test tube for Re=0.62 with D.C 1.5kV/mm

Fig. 18   Velocity distributions along the test tube for Re=0.62 with D.C 1.5kV/mm

The change in the flow rate of the ER fluid under an electric field of 1.5 kV/mm is shown in Fig. 16 ~ Fig. 18, as observed by PIV. At low flow velocity, the clusters build up from near the electrodes toward the tube center. With increasing flow speed the clusters at the tube center appear to break down. This breakdown is thought to be due to the inertia force, that is generated when the velocity increase is greater than the electric force among the starch particles, formed by ER effects. But near the electrodes, the viscosity effects of the
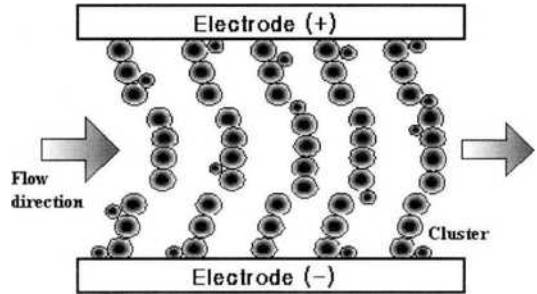

Fig. 19   Schematic clusters of ER fluid flow

ER fluid and the electric forces for the starch particle clusters are expected to be greater than the inertia forces so that the clusters may be broken down and their particles may be arranged toward the electrodes. The clusters, adhering to the electrodes become thicker and longer according to the intensity of the electric field. The clusters of the ER fluid, formed under flowing and coherence of clusters are resistant to fluid flows, and therefore, the fluid flows upstream at the upper part of the test tube after X/b=4.0.

ER fluid velocity is zero at the electrodes, and has a quadratic velocity profile at the other zone. Because of the clusters formed in these ways, the flow rate changes and the pressure of the ER fluid drops at the entrance and exit of the tube. ER fluid flowing along the test tube route changes the volume of the clusters, which are built up at the (+) and (−) electrodes, according to the intensity of the electric field. And it can be confirmed that a plug flow zone builds up at the center of the flow route. These phenomena are shown in Fig. 19. The results show that as the electric fields increase the cluster formations increase, the flow rate decreases, and Reynolds number decreases.

7. Conclusion

In this study, flow visualization experiments of ER fluid were performed ; the dislocations of particles were measured through image input devices, and; velocity distributions were obtained; The conclusions are as follows.

(1) If an electric field is formed around a stagnant ER fluid, bigger ER particles produce

more ER effects and shift toward (+) and (−) electrodes. The smaller stagnant particles may shift minutely because the bigger ones push their way through the smaller ones, and pressure increase and then, the voltex flow distributions appear. After positive and negative charges of ER particles are uniformly distributed and they reach equilibrium, and an electric field is formed, electric charges rotate toward the electrode having the opposite pole and build up momentum and have velocity vectors.

(2) The clusters, that adhere to the electrodes, become thicker and longer with the intensity of the electric field.

The clusters of the ER fluid, formed while flowing and the coherence of clusters make resistance against fluid flows. It confirmed that the velocity distribution and flow rate of ER fluid were changed by the intensity of the electric field.

(3) The band type clusters built up inside the flow route cannot maintain their shapes after the build up but repeat nullification and creation processes in short cycles. At low flow velocity, the clusters build up from near the electrodes toward the tube center. With increasing flow speed the clusters at the tube center appear to break down.

(4) ER fluid flowing along the test tube route change the volume of the cluster, which are built up at the (+) and (−) electrodes, according to the intensity of the electric field. And a plug flow zone builds up at the center of the flow route.

(5) The relationship between the Reynolds number and electric field shows with the increasing electric field, more cluster formation, decreasing the flow rate, and decreasing the Reynolds number.

Acknowledgments

Reference

Brooks D. A., 1992, "Design and Development of Flow Based Electro-Rheological Devices," Journal of Modern Physics, Vol. 6, pp. 2705~2730.

Choi S. B. and Cheong C. C., 1994, "Performance Investigation of a Cylinderical Valve Featuring Electro-Rheological Fluids," Korean Socity of Precision Engineering, Vol. 11, pp. 148~157.

Jang S. C., Yum M. O. and Kim D. T., 2001, "The Flow Characteristics of ER Fluids According to th Electrode Shape of Two Parallel-Plate," proceedings of the KSME 2001 Spring Annual Meeting E, pp. 207~212.

Jang S. C., Yum M. O. and Kim D. T., 2003, "Flow Rate-Pressure Drop Characteristics of Dispersive ER Fluid According to Change of Electric Field Strength in Clearance between Parallel Plates," KSMTE, Vol. 12, No. 1, pp. 78~83.

Jang S. C., Park C. S., Kim K. H. and Yum M. O., 2001, "The Flow Visualization of ER Fluid between Two Parallel-Plate Electrodes by Narrow Distance," KSMT, Vol. 3, No. 2, pp. 129~136.

Jeon Y. S., 1998, "Performance Investigation of Cylindrical-Type ER Valves With Different Electrode Length," Vol. 7, No. 6, pp. 1~11.

Nakano M. and Yonekawa T., 1994, "Pressure Response of ER Fluid in a Piston Cylinder ER Valve System," Proc. of the 4th Int. Conf. on Electrorheological Fluid, pp. 477~489.

Park M. K., Rhee E. J., Shuzo Oshi a and Ryuichiro Yamane, 1999, "The Flow Visualization of ER Fluid Between Two Parallel-Plate Electrodes Separated by Small Distance," KSME, Vol. 23, No. 7, pp. 801~810.

Simmonds A. J., 1991, "Electro-Rheological Valves in a Hydraulic Circuit," IEE Proceeding-D, Vol. 138, No. 4, pp. 400~404.

Tsukiji T., Takahashi J., Sugimoto H., Ikeda H., 1996, "Flow Characteris tics of ERF between Two Parallel-Plate Electrodes," JFPS, Vol. 25, No. 4, pp. 104~561.

Wang K. C., Mclay R. and Carey G. F., 1989, ER Fluid Modelling, CFD Laboratory, College of Engineering, University of Texas at Austin, Tx, USA. Proc. of the Second International Conference on ERF, pp. 41~52, 1989.

Yokota S., Kondoh Y., 1996, "A Control valve by Making use of an ER Fluid," JSME, Vol. 62, No. 601, pp. 93~100.